Article type

Research paper

Title

Investigating on relationship between effective quantum efficiency and irradiance

Zi-Piao Ye[1], Shuang-Xi Zhou[2], Xiao-Long Yang[3], Hua-Jing Kang[4], Piotr Robakowski[5]*

[1]*Math & Physics College, Jinggangshan University, Ji'an 343009, P. R. of China*; [2] *Department of Biological Sciences, Macquarie University, NSW 2109, Australia*; [3] *Department of Environmental Science and Engineering, Fudan University, Shanghai, 200433, China;* [4]*Wenzhou Vocational College of Science & Technology, Wenzhou 325006, P. R. of China; Department of Forestry, Poznan University of Life Sciences, Wojska Polskiego 71E St., 60–625 Poznan, Poland*;

Corresponding author(s)

Piotr Robakowski

Department of Forestry, Poznan University of Life Sciences, Wojska Polskiego 71E St., 60–625 Poznan, Poland

E-mail: pierrot@up.poznan.pl

Submitted to ***Journal of Experimental Botany***

Investigating on relationship between effective quantum efficiency and irradiance*

Zi-Piao Ye[1], Shuang-Xi Zhou[2*], Xiao-Long Yang[3], Hua-Jing Kang[4], Piotr Robakowski[5*]

[1]*Math & Physics College, Jinggangshan University, Ji'an 343009, P. R. of China*; [2] *Department of Biological Sciences, Macquarie University, NSW 2109, Australia*; [3] *Department of Environmental Science and Engineering, Fudan University, Shanghai, 200433, China;* [4]*Wenzhou Vocational College of Science & Technology, Wenzhou 325006, P. R. of China;* [5]*Department of Forestry, Poznan University of Life Sciences, Wojska Polskiego 71E St., 60–625 Poznan, Poland*

Highlight A model of the relationship between effective quantum efficiency of PS II (Φ_{PSII}) and irradiance (I) has been developed. Using this new model it was found that Φ_{PSII} decreased with increasing I due to the decrease in the effective absorption cross-section of photosynthetic pigments molecules.

Abstract Models describing the relationship between effective quantum efficiency of PS II (Φ_{PSII}) and irradiance (I) are routinely used to determine how irradiance influences effective quantum efficiency and photosynthetic electron transport rate (ETR). However, with no single model one can accurately describe the relationship between Φ_{PSII} and I, and explain the interdependence between Φ_{PSII} and biophysical properties of photosynthetic pigments, especially in plants growing under low level irradiances. Basing on the mechanistic model of photosynthetic electron transport rate we have developed the model of the relationship between Φ_{PSII} and I. The new model reveals that Φ_{PSII} increases with photochemistry (k_P) and heat dissipation (k_D). Furthermore, the values of key parameters calculated using the new model were compared with the values calculated with two other empirical models. The new model was perfectly fitted to the light-response curves of Φ_{PSII}. The key calculated photosynthetic parameters: maximum Φ_{PSII}, maximum ETR and their corresponding saturation irradiance were close to the measured values. In addition, our model associates Φ_{PSII} with intrinsic features of photosynthetic pigments. We concluded that Φ_{PSII} decreased with increasing I due to the decrease in the effective absorption cross-section of photosynthetic pigments molecules.

Keywords: Chlorophyll fluorescence, effective quantum efficiency, irradiance, photosynthetic electron transport rate, photosynthetic pigments, photosynthesis

* These authors contributed equally to this work.

Abbreviations

ETR Electron transport rate

ETR_{max} Maximum electron transport rate

F Steady-state fluorescence

F_m' Maximum fluorescence in the light

F_v Variable fluorescence yield of the dark-adapted leaf

g_i Degeneration of energy level of photosynthetic pigment molecules in the ground state *i*

g_k Degeneration of energy level of photosynthetic pigment molecules in the excited state *k*

I Irradiance

NPQ Non-photochemical quenching

N_0 Total light-harvesting pigment molecules

PAR_{sat} Saturation irradiance corresponding to ETR_{max}

k_P Rate of photochemical reaction

k_D Rate of non-radiative heat dissipation

PS II Photosystem II

a_e Initial slope of light-response curve of electron transport rate

α' Fraction of light absorbed by PS II

β' Leaf absorptance

ξ_1 Probability of photochemistry

ξ_2 Probability of non-radiative heat dissipation

ξ_3 Probability of fluorescence

σ_{ik} Eigen-absorption cross-section of photosynthetic pigment from ground state *i* to excited state *k* due to light illumination

σ'_{ik} Effective optical absorption cross-section of photosynthetic pigment molecule from ground state *i* to excited state *k* due to light illumination

φ Exciton-use efficiency in PS II

τ Average lifetime of the photosynthetic pigment molecules in the lowest excited state

Φ_{PSII} Effective quantum efficiency of PS II

Introduction

Light reactions of photosynthesis have been characterized by means of using the measurements of chlorophyll fluorescence as a useful and informative indicator (Krause & Weis, 1984; van Kooten & Snel, 1990; Rascher *et al*., 2000; van der Tol *et al*., 2014; Kalaji *et al*., 2016). The key photosynthetic parameters are: maximum quantum efficiency of photosystem II (F_v/F_m), effective quantum efficiency of photosystem II (Φ_{PSII}), photosynthetic electron transport rate (*ETR*) and other chlorophyll fluorescence parameters (e.g. non-photochemical quenching, *NPQ*, coefficient of photochemical quenching, *qL*). Genty *et al*. (1989) proposed that Φ_{PSII} at the steady state could be calculated from the ratio of the variable to maximum fluorescence in the light. It is a breakthrough concept of using fluorescence and irradiance (*I*) or the flux of photosynthetically active radiation (*PAR*) absorbed by leaf to estimate *ETR*, which is the most widely used to assess the efficiency of plants photochemistry in different environments (Genty *et al*., 1989; Majláth *et al*., 2016; Moin *et al*., 2016). Φ_{PSII} represents the proportion of photons of incident light that are actually used to drive photochemistry (Maxwell & Johnson, 2000). Φ_{PSII} is directly associated with *ETR* ($=\alpha' \times \beta' \times \Phi_{PSII} \times I$, where α' is a distribution coefficient of absorption of the light energy by PS II and PS I, β' is leaf absorptance, *I* is irradiance) (Krall & Edward, 1992). Under controlled conditions, this parameter linearly relates with quantum efficiency of CO_2 assimilation (Genty *et al*., 1989). However, in natural environment where stressors are likely to affect photosynthesis alternative processes to CO_2 assimilation, such as photorespiration or Mehler reaction may cause discrepancy between Φ_{PSII} and CO_2 assimilation (Fryer *et al*., 1998).

According to the definition of Φ_{PSII} [$\Phi_{PSII}=(F_m'-F)/F_m'$, where F_m' is maximum fluorescence in the light, *F* is steady-state fluorescence], it is clear that Φ_{PSII} is closely linked with the closure and opening of PS II in photosynthetic primary reactions as well as fluorescence emission of light-harvesting pigment molecules because chlorophyll fluorescence mainly come from these photosynthetic pigments (Baker, 2008). Photosynthesis research has long focused on Φ_{PSII} and *ETR* due to photosystem II (PS II) given its core role in photosynthesis, but also since PS II activity can be conveniently assayed via bio-optical techniques, e.g. chlorophyll fluorescence (e.g. Buckley & Farquhar, 2004; Robakowski, 2005; Baker, 2008; Suggett *et al*., 2010; Pavlovič *et al*., 2011). Numerous studies have used these fluorescence techniques to determine Φ_{PSII} and *ETR*

(see the references above) and found Φ_{PSII} to decrease nonlinearly with increasing irradiance (Robakowski, 2005; Pavlovič *et al*., 2011; van der Tol *et al*., 2014; Córdoba *et al*., 2016). However, no single model is currently able to describe satisfactorily the relationship between Φ_{PSII} and *PAR*, and reveal the action of intrinsic characteristics of light-harvesting pigments in Φ_{PSII}.

In photosynthesis, antenna pigment molecules absorb light energy to change the state of the pigments from the ground state to the excited state. Then, the excitation energy is mainly used by three inter-competing paths, i.e. photochemistry, heat dissipation and chlorophyll fluorescence emission (Müller *et al*., 2001; Oxborough, 2004; Baker, 2008). This competition among three de-excited paths (Oxborough, 2004; Baker, 2008) directly affects photosynthetic electron transport rates and formation of assimilation force (i.e. NADPH and ATP). Furthermore, light energy absorption, quantum state change, exciton resonant transfer among antenna pigment molecules and fluorescence emission in primary reaction are determined by intrinsic characteristics of the antenna pigment molecules (Govindjee, 2002; Baker, 2008; Richter *et al*., 2008 Panitchayangkoon *et al*., 2010; Sarovar *et al*., 2010). However, quantifying the nature of processes from light absorption to water splitting is still extremely limited but remains a key goal to improve models for predicting values of Φ_{PSII} from only light absorption measurements (Renk *et al*., 2000; Buckley & Farquhar, 2004).

As the research shows, methodologically, Φ_{PSII} can be directly modelled by several empirical models (Laws *et al*., 2002; Smyth *et al*., 2004; Ritchie, 2008; Ritchie & Bunthawin, 2010; Silsbe & Kromkamp, 2012) and is considered as an equivalent to *ETR*. Although these models can fit well light-response curves of electron transport rate (*ETR-I*) and light-response curves of effective quantum efficiency of PS II (Φ_{PSII}-*I*) under normal conditions, models simulating *ETR-I* and Φ_{PSII}-*I* in plants under low light intensities in greenhouse or under a forest trees' canopy are yet to be developed. Modelling of these curves under such irradiance environmental conditions is necessary for the evaluation of the generality of the models. Moreover, no previous model neither explains the reasons why Φ_{PSII} decreased nonlinearly with increasing irradiance (Robakowski, 2005; Pavlovič *et al*., 2011; van der Tol *et al*., 2014), nor helps to understand the way intrinsic characteristics of light-harvesting pigment molecules affect Φ_{PSII} and determine light harvesting, light energy conversion as well as subsequent productivity (*ETR*) through PS II.

In the present study, we hypothesized that: (1) Φ_{PSII} should be closely related to the intrinsic

properties of light-harvesting pigment molecules, closure and opening of PS II and photosynthetic enzyme kinetics of plants, (2) Φ_{PSII} depends on the competition of three paths of de-excitation, thus if more excitation energy is distributed to photochemistry, and less to heat dissipation, or chlorophyll fluorescence emission, Φ_{PSII} will be higher, and (3) behavior of the effective light absorption cross-section of light-harvesting pigment molecules will determine changes of Φ_{PSII}.

In this study, we firstly developed a model of the relationship between Φ_{PSII} and I based on fundamental properties of light absorption and transfer of energy to the reaction centers via photosynthetic pigment molecules (see Ye *et al*. 2013a, 2013b). Firstly, here we adopt a novel approach to determine the interdependence between the properties of photosynthetic pigments and Φ_{PSII} of plants under different light conditions. Secondly, we present the development of this model as applied to mung bean (*Vigna radiata* L.) under different light environments, and compare the fitted results with two empirical models which were introduced by Webb *et al*., (1974), Ritchie, (2008), and Smyth *et al*., (2004). Thirdly, we have evaluated these models for the relationship between Φ_{PSII} and I through comparing the fitted values of PAR_{sat} and ETR_{max}. Finally, we have investigated the impact of the intrinsic characteristics of light-harvesting pigment molecules on Φ_{PSII}.

MATERIALS AND METHODS

Study site and plants

At the end of June 2016, seeds of mung bean *Vigna radiata* [(L.) R. Wilczek] were soaked for 3 h and sowed on potted trays which were filled with matrixes (Scotts Miracle·Gro) consisted of turfy earth, coconut tree branny, pearlite and vermiculite and contained about 2.4 $g \cdot kg^{-1}$ of total nitrogen, 0.95 $g \cdot kg^{-1}$ of P_2O_5, 1.27 $g \cdot kg^{-1}$ of K_2O and about 0.71 $g \cdot kg^{-1}$ of trace elements. Seeds were germinated at the air temperature of 28 °C, the relative humidity of 80 % and light intensity of 125 μmol photons $m^{-2} \cdot s^{-1}$ (12h-day) and grown to the height of 7~10 cm. A total of 44 seedlings (healthy and uniform) were transplanted into 100 mm * 85 mm * 95 mm plastic pots, and divided randomly into four groups with 11 plants per group. They were cultured in phytotron with the day temperature of 25~28℃ and the

night temperature of 20~24℃. Three light regimes were established: LL (low light with 100 μmol photons $m^{-2} \cdot s^{-1}$), ML (middle light with 220 μmol photons $m^{-2} \cdot s^{-1}$), and HL (high light with 430 μmol photons $m^{-2} \cdot s^{-1}$). Plants were watered every morning up to the full substrate capacity. After 20 days, 5 healthy plants were randomly selected from each light treatment to measure their chlorophyll fluorescence parameters. When the plant height was about 20 cm, the third youngest fully expanded leaf from the top to bottom was used for fluorescence measurements (n = 5, n – number of replications).

Chlorophyll fluorescence measurements

Chlorophyll *a* fluorescence was measured on intact leaves using a chlorophyll fluorescence measuring system (Dual PAM-100, Walz, Effeltrich, Germany) with DUAL-E and DUAL-DB measuring heads. The initial level (F_0) of fluorescence was detected after 25 min of dark adaptation. The maximal fluorescence level (F_m) of the dark- and light- (F_m') adapted leaves were determined by applying saturating flashes (15.000 μmol photons $m^{-2} s^{-1}$) lasting 1 s, to promote the closure of the PS II reaction centers, according to the method described by Maxwell & Johnson (2000). The fluorescence parameters were calculated as described by van Kooten & Snel (1990) and Klughammer & Schreiber (2008). Maximum quantum efficiency of PS II, $F_v/F_m = (F_m - F_0)/F_m$; non-photochemical quenching, $NPQ = (F_m - F_m')/F_m'$. ETR was obtained as $ETR = \alpha' \times \beta' \times \Phi_{PSII} \times I$, where α' is distribution coefficient of absorption light energy by PS II and PSI to be assumed typically 0.5 (Maxwell & Johnson, 2000; Major & Dunton, 2002; Evans, 2009), leaf absorptance (β') is measured using an integrating sphere with a value typically returned of 0.86 (Ehleringer, 1981). Leaves were incrementally exposed to 14 irradiance levels (range 0 to 1450 μmol photons $m^{-2} s^{-1}$) at 30 s intervals.

Model 1

The photosynthetic electron transport rate via PS II can be described with Eq. 1 (Ye *et al.* 2013a, 2013b),

$$ETR = \frac{\alpha' \beta' N_0 \sigma_{ik} \varphi}{S} \times \frac{1 - \frac{(1 - g_i/g_k)\sigma_{ik}\tau}{\xi_3 + (\xi_1 k_P + \xi_2 k_D)\tau} I}{1 + \frac{(1 + g_i/g_k)\sigma_{ik}\tau}{\xi_3 + (\xi_1 k_P + \xi_2 k_D)\tau} I} I \quad (1)$$

where φ is exciton-use efficiency in PS II, N_0 is total photosynthetic pigment molecules of the measured leaf, S is the leaf area (m^2), g_i and g_k are the degeneration of energy levels of photosynthetic pigments in the ground state (i) and excited state (k), respectively. k_P and k_D are rates of the photochemical reaction and thermal deactivation, respectively. ξ_1, ξ_2 and ξ_3 are the occupation probability of photochemistry, non-radiation heat dissipation, and fluorescence emission, respectively. σ_{ik} is the eigen-absorption cross-section of photosynthetic pigments from the ground state i to excited state k via light exposure, τ is the average lifetime of the photosynthetic pigments in the lowest excited state k.

According to Ye et al., (2013a, 2013b), σ_{ik}, τ, ξ_1, ξ_2, ξ_3, g_i, g_k, k_P and k_D (Eq. 1) are inherently specific but have different values depending on species and environmental conditions (e.g. light, temperature, CO_2 concentration and relative humidity). Therefore, for a given species and at given environmental conditions, we can assume that $\alpha_e = \frac{\alpha' \beta' N_0 \sigma_{ik} \varphi}{S}$ (μmol electrons (μmol photons)$^{-1}$) is the initial slope of light-response curve of electron transport rate, $\beta_e = \frac{(1-g_i/g_k)\sigma_{ik}\tau}{\xi_3 + (\xi_1 k_P + \xi_2 k_D)\tau}$ (m^2 s (μmol photons)$^{-1}$) is the dynamical down-regulation term of PS II, and $\gamma_e = \frac{(1+g_i/g_k)\sigma_{ik}\tau}{\xi_3 + (\xi_1 k_P + \xi_2 k_D)\tau}$ (m^2 s (μmol photons)$^{-1}$) is the saturation term of photosynthesis. Eq. 1 can be simplified as,

$$ETR = \alpha_e \frac{1-\beta_e I}{1+\gamma_e I} I, \quad (2)$$

PAR_{sat} is calculated from Eq. 3,

$$PAR_{sat} = \frac{\sqrt{(\beta_e + \gamma_e)/\beta_e} - 1}{\gamma_e}, \quad (3)$$

Thus PAR_{sat} depends on σ_{ik}, τ, k_D, k_P, g_i, g_k, ξ_1, ξ_2 and ξ_3, but it is independent of N_0.

The maximum value for ETR (ETR_{max}) $= \alpha_e \frac{1-\beta_e \cdot PAR_{sat}}{1+\gamma_e \cdot PAR_{sat}} PAR_{sat}$, and it can be simplified as,

$$ETR_{max} = \alpha_e \left(\frac{\sqrt{\beta_e + \gamma_e} - \sqrt{\beta_e}}{\gamma_e} \right)^2, \quad (4)$$

Moreover, compared Eq. 1 with $ETR = \alpha' \times \beta' \times \Phi_{PSII} \times I$ (Krall & Edward, 1992), the relationship between Φ_{PSII} and I is described by Eq. 5,

$$\Phi_{PSII} = \frac{N_0 \sigma_{ik} \varphi}{S} \times \frac{1 - \frac{(1 - g_i/g_k)\sigma_{ik}\tau}{\xi_3 + (\xi_1 k_P + \xi_2 k_D)\tau} I}{1 + \frac{(1 + g_i/g_k)\sigma_{ik}\tau}{\xi_3 + (\xi_1 k_P + \xi_2 k_D)\tau} I}, \quad (5)$$

Eq. 5 demonstrates that Φ_{PSII} is closely related with intrinsic characteristics of light-harvesting pigment molecules, it does not only depend on I, but also on N_0, σ_{ik}, τ, φ, k_P, k_D, g_i, g_k, ξ_1, ξ_2 and ξ_3. In particular, Eq. 5 reveals that Φ_{PSII} increases with increasing k_P or k_D, and decreases with increasing τ. In addition, Eq. 5 can be simplified as:

$$\Phi_{PSII} = \frac{\alpha_e}{\alpha' \beta'} \frac{1 - \beta_e I}{1 + \gamma_e I}, \quad (6)$$

Eq. 6 shows clearly that Φ_{PSII} decreases non-linearly with increasing I at given environmental conditions (e.g. air temperature, CO_2 concentration and relative humidity).

In addition, the effective absorption cross-section of light-harvesting pigment molecules (σ'_{ik}) can also be expressed as a function of I (Ye *et al.*, 2013a, 2013b). Namely,

$$\sigma'_{ik} = \frac{\sigma_{ik}}{1 + \frac{(1 + g_i/g_k)\sigma_{ik}\tau I}{\xi_3 + (\xi_1 k_P + \xi_2 k_D)\tau}} \left[1 - \frac{(1 - g_i/g_k)\sigma_{ik}\tau I}{\xi_3 + (\xi_1 k_P + \xi_2 k_D)\tau} \right] \quad (7)$$

Eq. 7 shows that σ'_{ik} increases with k_P, k_D, ξ_1, ξ_2, ξ_3 and $1/\tau$ but decreases with I. $\sigma'_{ik} = \sigma_{ik}$ when $I = 0$. As such, the light absorption cross-section is not a constant under any given irradiance (excluding $I = 0$).

Compared Eq. 5 with Eq. 7, the relationship between Φ_{PSII} and σ'_{ik} is described by Eq. 8

$$\Phi_{PSII} = \frac{\alpha_e}{\alpha' \beta'} \times \frac{\sigma'_{ik}}{\sigma_{ik}} \quad (8)$$

Under given environmental conditions, the values of α_e, σ_{ik}, α' and β' are the constants. Therefore, Eq. 8 demonstrates that Φ_{PSII} is directly proportional to σ'_{ik} and it changes as a function of σ'_{ik}.

Model 2

Effective quantum efficiency of PSII (Φ_{PSII}) ranges from 0 to 1 (the maximum is not usually higher than 0.85). It has been found experimentally that Φ_{PSII} usually follows a simple

exponential decay function (Webb *et al*., 1974; Ritchie, 2008；Ritchie *et al*., 2010), namely,

$$\Phi_{PSII}=\Phi_{PSIImax}\times e^{-k_w I} \quad (9)$$

$\Phi_{PSIImax}$ is the maximum effective quantum efficiency which means the effective quantum efficiency at theoretical zero irradiance, k_w is a scaling constant, and I is the irradiance. The $\Phi_{PSIImax}$ can be obtained by Eq. 9.

Substituting Eq. 9 into $ETR=\alpha'\times\beta'\times\Phi_{PSII}\times I$ (Krall & Edward, 1992), we get the following expression for *ETR*:

$$ETR=\alpha'\times\beta'\times I\times\Phi_{PSIImax}\times e^{-k_w I} \quad (10)$$

Using Eq. 10, we can calculate saturation irradiance ($PAR_{sat}=1/k_w$) and maximum electron transport rate ($ETR_{max}=\alpha'\times\beta'\times PAR_{sat}\times\Phi_{PSIImax}\,e^{-1}$).

Here we take both Eqs. 9 and 10 as model 2.

Model 3

After Webb *et al*. (1974) introduced an exponential function, Smyth *et al*. (2004) and Silsbe & Kromkamp (2012) used this function to fit light-response curves of Φ_{PSII} (Eq. 11).

$$\Phi_{PSII}=\frac{F_v}{F_m}\times\frac{PAR_{sat}}{I}\left[1-\exp\left(-I/PAR_{sat}\right)\right], \quad (11)$$

F_v/F_m is the 'dark-adapted' maximum operating efficiency of PS II and PAR_{sat} is the saturation irradiance (Smyth *et al*., 2004). The F_v/F_m and PAR_{sat} can be obtained by Eq. 11.

Similarly, substituting Eq. 11 into $ETR=\alpha'\times\beta'\times\Phi_{PSII}\times I$ (Krall & Edward, 1992), we get the following expression for *ETR*,

$$ETR=\alpha'\times\beta'\times\frac{F_v}{F_m}\,PAR_{sat}\left[1-\exp\left(-I/PAR_{sat}\right)\right], \quad (12)$$

The maximum *ETR* can be calculated by the following formula,

$$ETR_{max}=\alpha'\times\beta'\times\frac{F_v}{F_m}\,PAR_{sat}\left[1-\exp\left(-1\right)\right] \quad (13)$$

Similarly, here we take Eqs. 12 and 13 as model 3.

Chlorophyll determination

Leaf discs from control areas were rapidly frozen in liquid nitrogen and ground to powder. Then the chlorophyll (Chl) was extracted with 80% (v/v) acetone and quantified with

spectrophotometer (*UVICON-930*, *Kontron Instruments*, Zürich, Switzerland). Chl *a* was determined at wavelength 663 nm, Chl *b* at 646 nm and carotenoids at 470 nm (Lichtenthaler 1987). Total chlorophyll content was determined as described by Porra, Thompson & Kriedermann (1989).

Statistical analysis

All variables are expressed as mean values (±SE) from five samples for each species. Data were analyzed with one-way analysis of variance (ANOVA) and then the values of ETR_{max} and PAR_{sat} estimated by three models were compared using a paired-sample *t* test at $\alpha < 0.05$ (α - significance level) using the SPSS 18.0 statistical software (SPSS, Chicago, IL). In addition, to compare the advantages and disadvantages of the study models, we took the Akaike's information criterion (*AIC*) and determination coefficient (R^2) as two indicators to assess the fitting results of the three models. AIC was calculated by reference to Akaike's method (1973), and R^2 was given directly by SPSS12.5 after fitting the data.

Results

Light-response curves of electron transport rate

Representative *ETR-I* curves (fitting the model 1, 2 and 3) for mung bean under three light environments are given in Fig. 1. In LL, *ETR* initially increased (almost linearly) with *I* towards saturation and subsequently, beyond the saturation irradiances exhibited a fast decline, suggesting dynamic down-regulation of PS II or photoinhibition (Fig. 1a). Under ML and HL, beyond PAR_{sat}, *ETR* values exhibited a little decline with increasing *I* (Fig. 1b and 1c). When the values of PAR_{sat} were compared among all the light environments, they ranged from 150 to 417 μmol photons m^{-2} s^{-1}. ETR_{max} followed a similar trend as PAR_{sat} and the values of ETR_{max} ranged from 7.36 to 26.04 μmol electrons m^{-2} s^{-1} given the little difference in initial slope of *J-I* curves ranging from 0.456 to 0.586 (Table 2). Moreover, it should be noted that under LL ETR_{max} (7.20±0.52 μmol electrons m^{-2} s^{-1}), PAR_{sat} (149.56±8.81 μmol photons m^{-2} s^{-1}) and the initial slope of *ETR-I* curve [ca. 0.456 μmol electrons (μmol photons)$^{-1}$] were lowest among three light environments. This result indicates that the capacity of light energy conversion of plants growing in LL is lower than in ML and in HL.

We used models 1, 2 and 3 to simulate light-response curves of electron transport rate of mung bean under three light environments. Fitted results showed that models 2 and 3 differed markedly from the measured data (Fig. 1). Under three light environments (LL, ML and HL), the coefficients of determination (R^2) for model 1 were 0.914, 0.828 and 0.982; for model 2 R^2 is 0.712, 0.223 and 0.592; for model 3 R^2 is 0.239, 0.792 and 0.955, respectively. Comparing the goodness of fit of the models, model 1, generally, had the best fit and showed greatest *AIC* values.

Under three light environments, the values of ETR_{max} and PAR_{sat} estimated by model 1 were in agreement with the measured data, whereas model 2 overestimated ETR_{max} and PAR_{sat}, and model 3 greatly underestimated ETR_{max} and PAR_{sat} (Table 1). ETR_{max} and PAR_{sat}, which are estimated by models 1, 2 and 3, R^2 and *AIC* derived from *ETR-I* curves (Fig. 1) are given in Table 1. Model 1 simulated well *ETR-I* curves, while models 2 and 3 fitted poorly *ETR-I* curves (Fig.1).

Light-response curves of Φ_{PSII}

Mung bean under three light environments exhibited a characteristic initial decrease of Φ_{PSII} with irradiance (Fig. 1). In LL, the decline of Φ_{PSII} differed significantly from HL and decreased more abruptly compared with the other light environments (Fig. 2). It indicates that plants growing in LL had the lowest light energy use efficiency to drive the photochemistry. Moreover, the simulations of the relationship between Φ_{PSII} and irradiance by model 1 are in perfect agreement with the experimental data ($R^2 \geq 0.985$) (Fig. 2).

In addition, the values of PAR_{sat} calculated by Eqs. 3 were not significantly different at a given light intensity (Table 2). Φ_{PSII} (and PAR_{sat}) calculated by Eqs. 9 (and 10) showed significant differences in each light environment (Table 3). Furthermore, Φ_{PSII} (and PAR_{sat}) calculated by Eqs. 11 and 12 differed significantly in each light environment (Table 4). For example, PAR_{sat} estimated by Eqs. 11 and 12 were 11.38 and 24.69 μmol photons $m^{-2} s^{-1}$ in LL, respectively. However, the measured value of PAR_{sat} was about 150 μmol photons $m^{-2} s^{-1}$.

Light-response curves of non-photochemical quenching (*NPQ*)

Representative *NPQ-I* curves for mung bean under three light environments are given in Fig. 3. Under LL and ML *NPQ* initially increased (almost linearly) with *I* and subsequently, at the middle irradiances (about 250 μmol photons $m^{-2} s^{-1}$), *NPQ* stabilized and then it increased with *I*.

In HL, *NPQ* increased fast when irradiances are beyond 250 μmol photons m^{-2} s^{-1} (Fig.3c). According to Eqn. (1), plants growing in HL have higher *ETR* than in LL and ML.

Light-response curves of effective light energy absorption cross-section

The potential for light-harvesting pigments to absorb light energy is reflected by the value of σ_{ik} which increases with the amount of light energy absorbed. For example, in LL, ML and in HL, σ_{ik} for mung bean calculated by $\sigma_{ik} = \frac{S\alpha_e}{\alpha' \beta' \varphi N_0}$ (where S is the measured leaf area, α_e is the initial slope of the light response of photosynthetic electron transport rate, α' is the fraction of light absorbed by photosystem II, β' is leaf absorptance, φ is excitation efficiency of PS II, i.e. for charge separation of P680) is (7.62±0.27) × 10^{-21} m^2, (9.85±0.46) × 10^{-21} m^2 and (11.65±0.68)×10^{-21} m^2, respectively; these values are all significantly different form one another (n = 5, one-way ANOVA followed by Tukey's test, α < 0.05). Eq. 7 shows that σ'_{ik} increases with k_p or k_D, but decreases (non-linearly) with increasing values of I, and/or τ. Therefore, the competition for each exciton amongst photochemistry, heat dissipation and fluorescence emission directly affects the effective light energy absorption cross-section of light-harvesting pigments (σ'_{ik}) (Fig. 4). At a given irradiance in σ'_{ik}–I curves, the higher σ'_{ik} is, the more light energy it absorbs. For example, in Fig. 4 at I= 600 μmol photons m^{-2} s^{-1} σ'_{ik} is 0.12×10^{-21} m^2, 0.26×10^{-21} m^2 and 0.36×10^{-21} m^2 under LL, ML and HL. It indicated that under HL mung bean had a higher ability to absorb light energy than under LL and ML.

Discussion

We have built a new model of the relationship between Φ_{PSII} and I based on light absorption and energy transfer to the reaction centers via photosynthetic pigments. It includes all relevant processes involving light energy absorption and conversion and transfer to the reaction centers of PS II (Ye *et al*., 2013a, 2013b).

The present study was focused on the relationships between Φ_{PSII}, *ETR*, σ_{ik} and I in mung bean seedlings growing in one of three light environments. Our main results were the Eq. 1 and 2 used to

determine *ETR* in function of *I* and explain the interdependence between *ETR* and biophysical parameters, such as σ'_{ik}. What is most important, we found that the Φ_{PSII} decrease is caused by the reduction of σ'_{ik} with increasing *I*. This finding is of fundamental importance to understand the molecular and biophysical mechanisms of variation in Φ_{PSII} under the changing light environment. In our study Φ_{PSII} not only depends on N_0, σ_{ik} and φ when environmental factors (e.g. irradiance, CO_2 concentration and temperature) are constant, but it depends also on τ, k_P, k_D, g_i, g_k, ξ_1, ξ_2 and ξ_3, specially on τ, k_P and k_D which are closely associated with processes of light energy absorption, excitons production and excitation energy transfer to reaction centers. In Eq. 5 Φ_{PSII} increases with k_P (Fig. 1) and k_D (Fig. 3) when they increase with light intensity, but Φ_{PSII} decreases with τ.

We used models 1, 2 and 3 to simulate *ETR-I* and Φ_{PSII}-*I* curves of mung bean in three light environmental conditions. There was evidence that model 2 and model 3 did not satisfactorily fit *ETR-I* and Φ_{PSII}-*I* curves. Generally, the values of PAR_{sat} and ETR_{max} estimated by model 2 were higher than the measured values (Table 2), while the values of PAR_{sat} and ETR_{max} estimated by model 3 were lower than the measured values (Table 2). These results were similar to Laws *et al.* (2002), Smyth *et al.* (2004), Silsbe & Kromkamp (2012). The values of PAR_{sat} and ETR_{max} estimated by model 1 were very close to the measured values (Table 2). Thus, we concluded that models 2 and 3 simulate poorly *ETR-I* and Φ_{PSII}-*I* curves, especially under high level of actinic light inducing dynamic down-regulation of PS II.

Mathematical models are not only useful to reproduce and explain the observed plants behavior, but also to make predictions and attempt to answer more fundamental questions. For example, model 1 (Eq. 5) forecasts increases in Φ_{PSII} with k_P and k_D, and decreases with increasing τ. Our results confirm that Φ_{PSII} increases with k_P and k_D. In HL k_P (reflected in *ETR*) and k_D (reflected in *NPQ*) (Table 2 and Fig. 3) were higher compared with LL and ML. What is of great importance, based on Eq. 5 or 8, the reason that Φ_{PSII} decreases with increasing *I* is the decrease in σ'_{ik}. In this study, in HL, mung bean shows the most abrupt decrease in σ'_{ik} compared with LL and ML (Fig. 4).

So far we have deliberately excluded that the environmental factors influence Φ_{PSII} to focus on properties of photosynthetic pigments and PSII which may have a significant effect on Φ_{PSII}. With the model presented here, it is straightforward to include equations representing *ETR-I* and

398 Φ_{PSII}-I which are associated with light energy absorption, excitons production and its transfer to
399 photochemical reaction centers, which may answer why LL mung bean has the lowest Φ_{PSII},
400 ETR_{max} and PAR_{sat} values, and also explain why its ETRs decline fastest compared with ML and
401 HL plants. If the model of the relationship between Φ_{PSII} and I is combined with Eq. 1 (Ye *et al*.
402 2013a), much information on physical and biochemical parameters of photosynthetic pigments
403 could be obtained. Additionally, the model of the relationship between Φ_{PSII} and I indicates Φ_{PSII}
404 to be proportional to the product of N_0, φ and σ_{ik} besides τ, k_P, k_D, g_i, g_k, ξ_1, ξ_2 and ξ_3. Therefore,
405 plants with a higher product of N_0, φ and σ_{ik} have a higher initial value of Φ_{PSII}.

406 In conclusion, the proposed model provides the means to predict and simulate the Φ_{PSII}-I
407 curves. The Φ_{PSII} decrease with increasing I stems from the decrease in effective light energy
408 absorption cross-section of photosynthetic pigments (see Ye *et al*., 2013a, 2013b). When the
409 presented model is combined with the mechanistic model of *ETR*-*I*, they could become an
410 effective tool towards identifying novel mechanistic properties by which plants modify their light
411 harvesting properties and show photoacclimation (Dubinsky & Stambler, 2009), photoprotection
412 (Takahashi & Badger, 2011; Niyogi & Truong, 2013), dynamic down-regulation of PSII (Ralph &
413 Gademann, 2005) or photoinhibition (Govdjee, 2002) in response to environmental stressors. A
414 cutting-edge next step will be to investigate more species adapted to different environmental
415 conditions along geographical gradients to distinguish between genetic and environmental factors
416 effects on Φ_{PSII}.

417

418 **Acknowledgements**

419 This research was supported by the Natural Science Foundation of China (Grant No. 31560069)
420 and the Natural Science Foundation of Jiangxi Province (Grant No. 20142BAB20402).

References

Baker NR. 2008. Chlorophyll fluorescence: A probe of photosynthesis in vivo. Annual of Review Plant Biology **59,** 89–113.

Buckley TN, Farquhar GD. 2004. A new analytical model for whole-leaf potential electron transport rate. Plant, Cell and Environment **27,** 1487–1502.

Córdoba J, Molina-Cano J-L, Martínez-Carrasco R, Morcuende R, Pérez P. 2016. Functional and transcriptional characterization of a barley mutant with impaired photosynthesis. Plant Science **244,** 19–30.

Dubinsky Z, Stambler N. 2009. Photoacclimation processes in phytoplankton: mechanisms, consequences, and applications. Aquatic Microbial Ecology **56,** 163–176.

Ehleringer JR. 1981. Leaf absorptances of Mohave and Sonoran deserts plants. Oecologia **49,** 366–370.

Evans JR. 2009. Potential error in electron transport rates calculated from chlorophyll fluorescence as revealed by multilayer leaf model. Plant and Cell Physiology **50,** 698–706.

Fryer MJ, Andrews JR, Oxborough K, Blowers DA, Baker NR. 1998. Relationship between CO_2 assimilation, photosynthetic electron transport, and active O_2 metabolism in leaves of maize in the field during periods of low temperature. Plant Physiology **116,** 571-580.

Genty B, Briantais JM, Baker NR. 1989. The relationship between the quantum efficiency of photosynthetic electron transport and quenching of chlorophyll fluorescence. Biochimica et Biophysica Acta **990,** 87–92.

Govindjee 2002. A role for a light-harvesting antenna complex of photosystem II in photoprotection. Plant Cell **14,** 1663–1668.

Kalaji HM, Jajoo A, Oukarroum A, Brestic M, Zivcak M, Samborska IA, Cetner MD, Łukasik I, Goltsev V, Ladle RJ. 2016. Chlorophyll a fluorescence as a tool to monitor physiological status of plants under abiotic stress conditions. Acta Physiologiae Plantarum **38,** 102.

Klughammer C, Schreiber U. 2008. Complementary PS II quantum yields calculated from simple fluorescence parameters measured by PAM fluorometry and the saturation pulse method. PAM Application Notes **1,** 11–14

Krall JP, Edward GE. 1992. Relationship between photosystem II activity and CO_2 fixation in leaves. Physiologia Plantarum **86,**180–187.

Krause GH, Weis E. 1984. Chlorophyll fluorescence as a tool in plant physiology. II. Interpretation of fluorescence signals. Photosynth Research **5,** 139–157

Laws E, Sakshaug E, Babin M, Dandonneau Y, Falkowski P, Geider R, Legendre L, Morel A, Sondergaard M, Takahashi M, Williams PJ. 2002. Photosynthesis and primary productivity in marine ecosystems: Practical aspects and application of techniques. JGOFS Report No. 36.

Lichtenthaler HK. 1987. Chlorophyll and carotenoids - pigments of photosynthetic biomembranes. Method in Enzymology **148,** 350–382.

Majláth I, Darko E, Palla B, Nagy Z, Janda T, Szalai G. 2016. Reduced light and moderate water deficiency sustain nitrogen assimilation and sucrose degradation at low temperature in durum wheat. Journal of Plant Physiology **191,** 149–158.

Major KM, Dunton KH. 2002. Variations in light-harvesting characteristics of the seagrass, *Thalassia testudinum*: evidence for photoacclimation. Journal of Experimental Marine Biology and Ecology **275,** 173–189.

Maxwell K, Johnson NG. 2000. Chlorophyll fluorescence—a practical guide. Journal of Experimental Botany **51,**

659–668.

Moin M, Bakshi A, Saha A, Kumar MU, Reddy AR, Rao KV, Siddiq EA, Kirt PB. 2016. Activation tagging in Indica rice identifies ribosomal proteins as potential targets for manipulation of water-use efficiency and abiotic stress tolerance in plants. Plant, Cell and Environment **39,** 2440–2459.

Niyogi KK and Truong TB. 2013. Evolution of flexible non-photochemical quenching mechanisms that regulate light harvesting in oxygenic photosynthesis. Current Opinion in Plant Biology **16,** 307–314.

Oxborough K. 2004. Imaging of chlorophyll a fluorescence: theoretical and practical aspects of an emerging technique for the monitoring of photosynthetic performance. Journal of Experimental Botany **55,** 1195-1205.

Panitchayangkoon G, Hayes D, Fransted KA, Caram JR, Harel E, Wen J, Blankenship RE, Engel GS. 2010. Long-lived quantum coherence in photosynthetic complexes at physiological temperature. Proceedings of National Academy of Sciences of the United States of America **107,** 12766-12770.

Pavlovič A, Slováková L, Pandolfi C, Mancuso S. 2011. On the mechanism underlying photosynthetic limitation upon trigger hair irritation in the carnivorous plant venus flytrap (*Dionaea muscipula* Ellis). Journal of Experimental Botany **62,** 1991–2000.

Porra RJ, Thompson WA, Kriedermann PE. 1989. Determination of accurate extinction coefficient and simultaneous equations for essaying chlorophylls a and b extracted with four different solutions: verification of the concentration of chlorophyll standards by atomic absorption spectroscopy. Biochemica and Biophysica Acta **975,** 384–394.

Ralph PJ, Gademann R. 2005. Rapid light curves: A powerful tool assess photosynthetic activity. Aquatic Botany **82,** 222–237.

Rascher U, Liebieg M, Lüttge U. 2000. Evaluation of instant light-response curves of chlorophyll fluorescence parameters obtained with a portable chlorophyll fluorometer on site in the field. Plant, Cell and Environment **23,** 1397–1405.

Renk H, Ochocki S, Kurzyk S. 2000. *In situ* and *simulated in situ* primary production in the Gulf of Gdańsk. Oceanologia **42,** 263–282.

Richter M, Renger T, Knorr A. 2008. A Block equation approach to intensity dependent optical spectra of light harvesting complex II. Photosynthesis Research **95,** 119–127.

Ritchie RJ. 2008. Fitting light saturation curves measured using modulated fluorometry. Photosynthesis Research **96,** 201–215.

Ritchie RJ, Bunthawin S. 2010. The use of pulse amplitude modulation (PAM) fluorometry to measure photosynthesis in a cam orchid, *Dendrobium* spp. (D. cv. *Viravuth pink*). International Journal of Plant Science **171,** 575–585.

Robakowski P. 2005. Susceptibility to low-temperature photoinhibition in three conifers differing in successional status. Tree Physiology **25,** 1151–1160.

Sarovar M , Ishizaki A , Fleming GR , Whaley KB. 2010. Quantum entanglement in photosynthetic light-harvesting complexes. Nature Physics **6,** 462-467.

Silsbe GM, Kromkamp JC. 2012. Modeling the irradiance dependency of the quantum efficiency of photosynthesis. Limnology and Oceanography: Methods **10,** 645–652.

Smyth TJ, Pemberton KL, Aiken J, Geider RJ. 2004. A methodology to determine primary production and

phytoplankton photosynthetic parameters from Fast Repetition Rate Fluorometry. Journal of Plankton Research **26,** 1337–1350.

Suggett DJ, Prasil O, Borowitzka MA. 2010. Chlorophyll *a* fluorescence in aquatic sciences: methods and applications (developments in applied phycology). Springer, London, pp 323.

Takahashi S, Badger MR. 2011. Photoprotection in plants: a new light on photosystem II damage. Trends in Plant Science **16,** 53–59.

van der Tol C, Berry JA, Campbell PKE, Rascher U. 2014. Models of fluorescence and photosynthesis for interpreting measurements of solar-induced chlorophyll fluorescence, Journal of Geophysical Research: Biogeosciences **119,** 2312–2327.

van Kooten O, Snel JFH. 1990. The use of chlorophyll fluorescence nomenclature in plant stress physiology. Photosynthesis Research **25,** 147–150.

Ye ZP, Robakowski P, Suggett DJ. 2013a. A mechanistic model for the light response of photosynthetic electron transport rate based on light harvesting properties of photosynthetic pigment molecules. Planta **237,** 837–847.

Ye ZP, Suggett DJ, Robakowski P, Kang HJ. 2013b. A mechanistic model for the photosynthesis-light response based on the photosynthetic electron transport of PSII in C_3 and C_4 species. New Phytologist **199,** 110–120.

Tables

Table 1. Measured data and results fitted by three models for *ETR-I* curves of mung bean under three light environments. ETR_{max} and PAR_{sat} estimated by three models were compared using a paired-sample *t* test at $\alpha < 0.05$ (α - significance level); the values followed by the different superscript letters are significantly different among three models in each light environment. All values indicate the mean ±SE ($n = 5$) except measured data.

Photosynthetic parameters	100 μmol photons $m^{-2} s^{-1}$				200 μmol photons $m^{-2} s^{-1}$				340 μmol photons $m^{-2} s^{-1}$			
	Model 1	Model 2	Model 3	Measured data	Model 1	Model 2	Model 3	Measured data	Model 1	Model 2	Model 3	Measured data
PAR_{sat}(μmol photons m^{-2} s^{-1})	149.56 ±8.81^{b}	191.86 ±13.26^{a}	11.38 ±1.13^{c}	≈150	249.98 ±12.56^{b}	304.62 ±10.05^{a}	21.11 ±1.04^{c}	≈250	447.01 ±20.80^{a}	470.89 ±11.72^{a}	52.88 ±1.10^{b}	≈437
ETR_{max}(μmol electrons m^{-2} s^{-1})	7.20 ±0.52^{b}	9.37 ±0.70^{a}	3.02 ±0.30^{c}	≈7.36	9.90 ±0.32^{b}	13.53 ±0.41^{a}	5.60 ±0.28^{c}	≈10.25	26.07 ±1.17^{b}	32.89 ±1.36^{a}	13.84 ±0.26^{c}	≈26.04
R^2	0.914 ±0.009	0.712 ±0.008	0.239 ±0.005	-	0.948 ±0.004	0.223 ±0.009	0.792 ±0.002	-	0.982 ±0.005	0.592 ±0.024	0.955 ±0.004	-
AIC	-18.51	-20.23	-13.17		-9.92	-0.15	-33.73		16.70	17.34	-19.10	

Table 2 Measured data and results fitted by model 1 for *ETR-I* and Φ_{PSII}-*I* of mung bean under three light environments. The values of ETR_{max} and PAR_{sat} estimated by model 1 were compared using a paired-sample *t* test at $\alpha < 0.05$ (α - significance level); the values followed by the different superscript letters are significantly different in each light environment. All values indicate the mean ± SE ($n = 5$) except measured data.

Photosynthetic parameters	100 μmol photons $m^{-2} s^{-1}$			200 μmol photons $m^{-2} s^{-1}$			340 μmol photons $m^{-2} s^{-1}$		
	Model 1			Model 1			Model 1		
	Φ_{PSII}-*I*	*ETR-I*	Measured data	Φ_{PSII}-*I*	*ETR-I*	Measured data	Φ_{PSII}-*I*	*ETR-I*	Measured data
$\Phi_{PSIImax}$	0.742 ±0.016	-	-	0.772 ±0.012	-	-	0.756 ±0.019	-	-
PAR_{sat}	161.19 ±12.75[a]	149.56 ±8.82[a]	≈150	285.06 ±8.62[a]	249.98 ±12.56[a]	≈250	396.36 ±6.90[a]	447.01 ±20.80[a]	≈437
ETR_{max}	-	7.20 ±0.52	≈7.36	-	9.90 ±0.32	≈10.25	-	26.07 ±1.17	≈26.04
R^2	0.998 ±0.005	0.914 ±0.009	-	0.996 ±0.004	0.948 ±0.004	-	0.985 ±0.013	0.954 ±0.005	-

Table 3 Measured data and results fitted by model 2 for *ETR-I* and Φ_{PSII}-*I* of mung bean under three light environments. ETR_{max}, PAR_{sat} and $\Phi_{PSIImax}$ estimated by model 2 were compared using a paired-sample *t* test at $\alpha < 0.05$ (α - significance level); the values followed by the different superscript letters are significantly different in each light environment. All values indicate the mean ±SE ($n = 5$) except measured data.

Photosynthetic parameters	100 μmol photons $m^{-2} s^{-1}$			200 μmol photons $m^{-2} s^{-1}$			340 μmol photons $m^{-2} s^{-1}$		
	Model 2			Model 2			Model 2		
	Φ_{PSII}-*I*	*ETR-I*	Measured data	Φ_{PSII}-*I*	*ETR-I*	Measured data	Φ_{PSII}-*I*	*ETR-I*	Measured data
$\Phi_{PSIImax}$	0.703 ±0.015[a]	0.316 ±0.012[b]	-	0.759 ±0.004[a]	0.288 ±0.010[b]	-	0.758 ±0.006[a]	0.454 ±0.026[b]	-
PAR_{sat}	65.08 ±10.05[b]	191.86 ±13.26[a]	≈150	147.64 ±5.47[b]	304.62 ±10.05[a]	≈250	238.28 ±12.91[b]	470.89 ±11.72[a]	≈437
ETR_{max}	-	9.37 ±0.70	≈7.2	-	13.53 ±0.41	≈10.25	-	32.89 ±1.36	26.04
R^2	0.983 ±0.011	0.776 ±0.054	-	0.989 ±0.005	0.226 ±0.051	-	0.991 ±0.003	0.652 ±0.025	-

Table 4 Measured data and results fitted by model 3 for *ETR-I* and Φ_{PSII}-*I* curves of mung bean under three light environments. ETR_{max} and PAR_{sat} estimated by model 3 were compared using a paired-sample *t* test at $\alpha < 0.05$ (α - significance level); the values followed by the superscript letters are significantly different in each light environment. All values indicate the mean±SE ($n = 5$) except measured data.

Photosynthetic parameters	100 μmol photons $m^{-2} s^{-1}$			200 μmol photons $m^{-2} s^{-1}$			340 μmol photons $m^{-2} s^{-1}$		
	Model 3			Model 3			Model 3		
	ETR-I	Φ_{PSII}-*I*	Measured data	*ETR-I*	Φ_{PSII}-*I*	Measured data	*ETR-I*	Φ_{PSII}-*I*	Measured data
$\Phi_{PSIImax}$	-	-	-	-	-	-	-	-	-
PAR_{sat}	11.38 ±1.13^{b}	24.69 ±1.41^{a}	≈150	21.11 ±1.04^{b}	52.61 ±1.84^{a}	≈250	52.88 ±1.10^{b}	103.01 ±4.49^{a}	≈417
ETR_{max}	3.02 ±0.030	-	≈7.2	5.60 ±0.28	-	≈10.25	13.84 ±0.26	-	≈26.04
R^2	0.301 ±0.048	0.995 ±0.008	-	0.795 ±0.025	0.996 ±0.003	-	0.959 ±0.006	0.984 ±0.016	-

Captions of figures

Figure 1. Light-response curves of electron transport rate of mung bean under three light environments (a, LL - 100, b, ML - 200 and c, HL - 340 μmol photons $m^{-2} s^{-1}$) and the curves simulated by models 1, 2 and 3 .

Figure 2. Light-response curves of effective quantum efficiency (Φ_{PSII}) of mung bean under three light environments (a, LL - 100, b, ML - 200 and c, HL - 340 μmol photons $m^{-2} s^{-1}$) and the curves simulated by models 1, 2 and 3.

Figure 3. Light-response curves of non-photochemical quenching (*NPQ-I*) of mung bean under three light environments (a, LL - 100, b, ML - 200 and c, HL - 340 μmol photons $m^{-2} s^{-1}$).

Figure 4. Light-response curves of effective light energy absorption cross-section (σ'_{ik} -*I*) of mung bean under three light environments (a, LL - 100, b, ML - 200 and c, HL - 340 μmol photons $m^{-2} s^{-1}$).

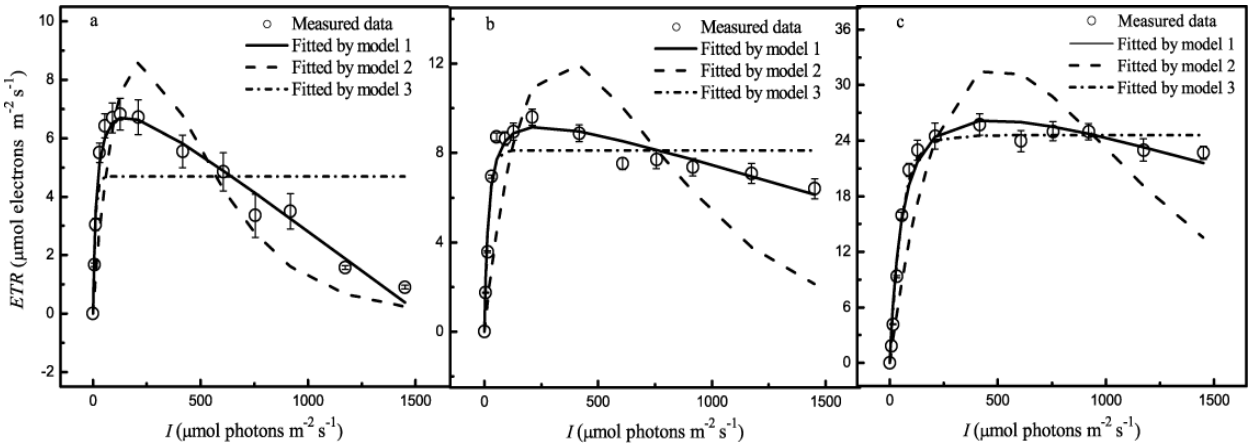

Figure 1

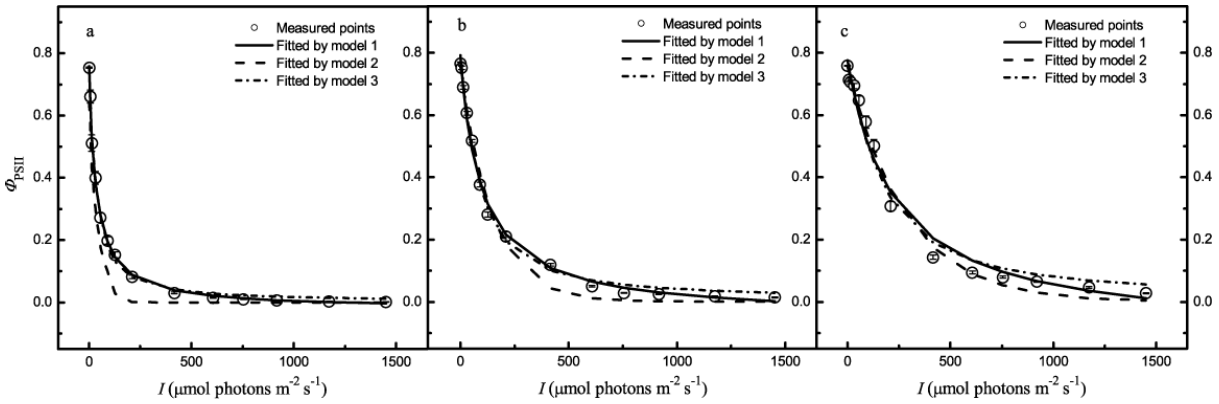

Figure 2

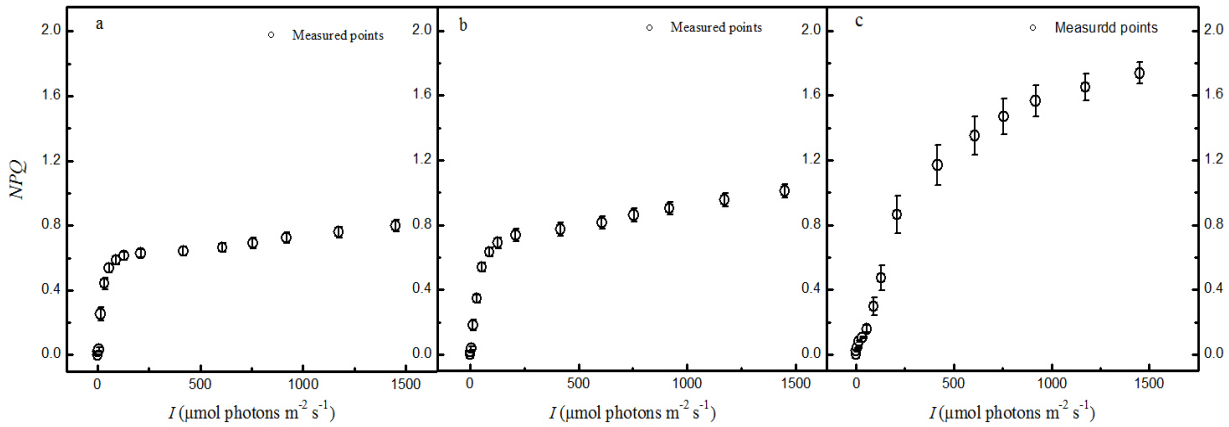

Figure 3

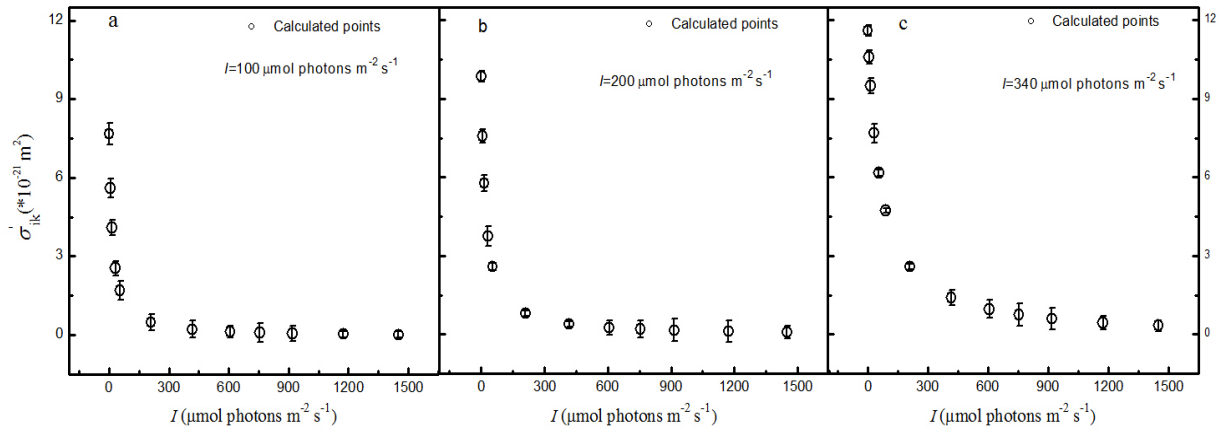

Figure 4